ResearchGate

See discussions, stats, and author profiles for this publication at: https://www.researchgate.net/publication/8559353

Conformation and Dynamics of Ribosomal Stalk Protein L12 in Solution and on the Ribosome †

ARTICLE *in* BIOCHEMISTRY · JUNE 2004

Impact Factor: 3.02 · DOI: 10.1021/bi0495331 · Source: PubMed

CITATIONS
49

READS
15

7 AUTHORS, INCLUDING:

Lamine Bouakaz
Novartis
10 PUBLICATIONS **222** CITATIONS
SEE PROFILE

Anders Liljas
Lund University
147 PUBLICATIONS **7,171** CITATIONS
SEE PROFILE

Mikael Akke
Lund University
102 PUBLICATIONS **5,453** CITATIONS
SEE PROFILE

Suparna Sanyal
Uppsala University
46 PUBLICATIONS **748** CITATIONS
SEE PROFILE

Available from: Suparna Sanyal
Retrieved on: 30 January 2016

Accelerated Publications

Conformation and Dynamics of Ribosomal Stalk Protein L12 in Solution and on the Ribosome†

Frans A. A. Mulder,‡ Lamine Bouakaz,§ Anna Lundell,|| Musturi Venkataramana,§ Anders Liljas,|| Mikael Akke,*,‡ and Suparna Sanyal*,§

Department of Biophysical Chemistry, Lund University, Box 124, SE-22100 Lund, Sweden, Department of Cell and Molecular Biology, BMC, Uppsala University, Box 596, SE-75124 Uppsala, Sweden, and Department of Molecular Biophysics, Lund University, Box 124, SE-22100 Lund, Sweden

Received March 9, 2004; Revised Manuscript Received April 8, 2004

ABSTRACT: During translation, the ribosome and several of its constituent proteins undergo structural transitions between different functional states. Protein L12, present in four copies in prokaryotic ribosomes, forms a flexible "stalk" with key functions in factor-dependent GTP hydrolysis during translocation. Here we have used heteronuclear NMR spectroscopy to characterize L12 conformation and dynamics in solution and on the ribosome. Isolated L12 forms a symmetric dimer mediated by the N-terminal domains (NTDs), to which each C-terminal domain (CTD) is connected via an unstructured hinge segment. The overall structure can be described as three ellipsoids joined by flexible linkers. No persistent contacts are seen between the two CTDs, or between the NTD and CTD in the L12 dimer in solution. In the $^{1}H-^{15}N$ HSQC spectrum of the *Escherichia coli* 70S ribosome, a single set of cross-peaks are observed for residues 40−120 of L12, the intensities of which correspond to only two of four protein copies. The structure of the CTDs observed on the ribosome is indistinguishable from that of isolated L12. These results indicate that two CTDs with identical average structures are mobile and extend away from the ribosome, while the other two copies most likely interact tightly with the ribosome even in the absence of translational factors.

In the past few years, structural studies by X-ray crystallography and cryoelectron microscopy (cryo-EM) have made dramatic progress in understanding the function of the ribosome at the level of (near) atomic detail (*1*−*5*). Protein synthesis involves the action of different translation factors, which catalyze the different steps of translation, viz., initiation, elongation, termination, and recycling. These protein factors bind transiently to the ribosome where they undergo conformational transitions (*6*−*8*). Certain parts of the ribosome are also inherently flexible, and the dynamic properties of these parts are in many cases critical for the proper function of the ribosome (*7*−*9*). Clearly, the protein synthesis machinery is a highly dynamic system. As increasingly more structural information on the ribosome becomes available, the focus of the field is gradually shifting toward understanding the detailed motions necessary to accomplish translation (*9*−*11*).

Prokaryotic ribosomal protein L12 is involved in the binding and GTP hydrolyzing activity of translational GTPases (*12*−*15*), and in the control of translation accuracy (*16*−*18*). Functionally analogous, but nonhomologous, proteins are present in eukaryotes and archaea (*19*). L12 forms a prominent "stalk"-like protuberance on the 50S subunit, as observed by cryo-EM (*20*). Notably, the L12 analogue is not visible in the 2.4 Å crystal structures of the 50S particle (*1*), and is highly disordered in the high-resolution structure of the 70S particles (*5*, *21*). A large body of structural and biochemical data has suggested that parts of ribosome-bound L12 are mobile (*22*−*24*), and that its conformation and flexibility are dramatically altered upon binding of translation factors EF-G (*8*, *20*, *25*) and EF-Tu (*7*, *26*) to the ribosome. Evidence from chemical cross-linking (*27*) and immuno-EM (*28*) studies shows that the CTD[1] contacts different parts of the ribosome, including the 30S neck and head regions, as well as a position close to the EF-G binding site near L10 (*29*).

† Supported by research grants from the Swedish Research Council to M.A., S.S., and A. Liljas, from the Swedish Foundation for Strategic Research to M.A., and from the EU-4th framework to A. Liljas. F.A.A.M. was supported by a Marie Curie fellowship (HPMF-CT-2001−01245) awarded by the European Commission.

* To whom correspondence should be addressed. M.A.: e-mail, mikael.akke@bpc.lu.se; phone, +46-46-2228247; fax, +46-46-2224543. S.S.: e-mail, suparna.sanyal@icm.uu.se; phone, +46-18-4714220; fax, +46-18-4714262.

‡ Department of Biophysical Chemistry, Lund University.

§ Uppsala University.

|| Department of Molecular Biophysics, Lund University.

[1] Abbreviations: CTD, C-terminal domain; NTD, N-terminal domain; HSQC, heteronuclear single-quantum coherence; NMR, nuclear magnetic resonance; SDS−PAGE, sodium dodecyl sulfate−polyacrylamide gel electrophoresis.

10.1021/bi0495331 CCC: $27.50 © 2004 American Chemical Society
Published on Web 04/27/2004

L12 is the only component of the ribosome that is present in multiple copies, being arranged as two dimers bound to protein L10, which in turn is bound to the 23S rRNA. L12 consists of an N-terminal domain (NTD, residues 1−31) that is responsible for dimerization and binding to protein L10 (*30*−*32*), a C-terminal domain (CTD, residues 52−120) that is required for interactions with translation factors (*30*, *32*), and a flexible hinge region (residues 32−51) that enables movement of the CTDs relative to the NTDs, a property that is required for ribosome activity (*18*, *33*, *34*). Small-angle X-ray scattering and fluorescence polarization have shown that isolated *Escherichia coli* L12 is a tightly associated and highly elongated dimer in solution (*24*, *35*). High-resolution crystal structures are available for the isolated CTD of *E. coli* L12 (*36*), as well as for two intact L12 molecules in association with two proteolytic NTD fragments from *Thermotoga maritima* (*37*). The latter structure revealed two different dimerization modes, and it was proposed that these might reflect structural variants of functional relevance (*11*, *37*). Very recently, an NMR solution structure of the L12 dimer was reported (*38*), which agrees well with earlier observations and predictions (*11*, *39*).

A number of remaining questions are related to the function of L12 in translation. How many copies of L12 form the ribosomal stalk? How are the L12 dimers oriented on the ribosome? Is the structure of the L12 dimer dramatically altered when bound to the ribosome? Which parts of L12 are flexible when bound to the ribosome? The answers to these questions are critical for understanding the functional role of L12 in translation. Here we have addressed these questions using $^{1}H-^{15}N$ NMR spectroscopy. Our results provide residue-specific information about the conformation and dynamics of L12 free in solution and bound to the ribosome. Combining our novel observations with published structural data for L12, we suggest two possible arrangements of L12 dimers on the ribosome.

MATERIALS AND METHODS

NMR Sample Preparation. *E. coli* ribosomal protein L12, cloned in plasmid pET24b, was overexpressed in *E. coli* BL21(DE3), in $^{15}NH_4Cl$-containing minimal medium by IPTG induction at an OD_{595} of 0.6. Purification was performed following published protocols (*40*) with minor modifications. The pure protein was dialyzed in 10 mM Tris buffer (pH 6.8) containing 30 mM potassium chloride, 10 mM magnesium chloride, 10 mM ammonium chloride, 0.5 mM EDTA, 1 mM DTT, and a 93/7 (v/v) H_2O/D_2O mixture. The concentration of the ^{15}N-labeled L12 sample used for NMR was between 8 and 10 mg/mL, as measured by the Bradford assay. For comparison with ribosome spectra (see below), one L12 sample was prepared in the same buffer described above at pH 7.3.

Ribosomes uniformly enriched in ^{15}N were obtained from *E. coli* MRE600 cells grown in minimal medium containing $^{15}NH_4Cl$, and were purified according to published protocols (*41*) with minor modifications. These ^{15}N-labeled ribosomes were highly active (>85%) as measured by *in vitro* dipeptide synthesis. The final sucrose density gradient centrifugation step resolved the 50S and 70S peaks, which were collected separately and resuspended in polymix buffer at pH 7.3 (*42*). The concentrations of the ^{15}N-labeled 70S and 50S samples used in this study were 11.2 and 16.6 μM, respectively, as measured from the absorbance at 260 nm (*43*). The integrity of the 70S ribosome sample was verified using size-exclusion chromatography on a Superdex-200 analytical column and high-density Phast SDS−PAGE.

NMR Spectroscopy. All experiments were performed at 30.0 ± 0.1 °C on a Varian Unity Inova 600 MHz spectrometer equipped with an inverse broadband probehead and single-axis pulsed-field gradient capabilities. Spectra were typically recorded with spectral widths of 12 000 Hz, sampled over 1536 complex points, in the ^{1}H dimension and 2000 Hz, sampled over 128 complex points, in the ^{15}N dimension. Published chemical shift assignments of L12 (*44*) were transferred to the current experimental conditions using three-dimensional (3D) $^{1}H-^{15}N$ TOCSY-HSQC and 3D $^{1}H-^{15}N$ NOESY-HSQC experiments (*45*).

^{15}N longitudinal (R_1) and transverse (R_2) relaxation rates and $\{^{1}H\}-^{15}N$ NOEs were measured using pulse sequences described previously (*46*). The R_1 relaxation delays were 150, 230, 330 (3), 560, 750 (2), and 1000 ms, and the R_2 delays were 10, 38 (2), 60, 85, 120 (2), 180 (2), and 220 ms, where (2) and (3) indicate duplicate and triplicate experiments, respectively. The $\{^{1}H\}-^{15}N$ NOE values were determined as the ratio of the peak intensities from two spectra recorded with and without a 5 s ^{1}H saturation period incorporated at the end of a 12 s delay between each pulse sequence repetition. The two spectra were recorded in an interleaved manner to ensure identical conditions in the two experiments. Transverse cross-relaxation rates (η_{xy}) due to cross correlation between the dipolar and chemical shift anisotropy relaxation mechanisms were measured as described previously (*47*). The number of transients recorded in the cross and reference experiments was 48 and 16, respectively. The η_{xy} relaxation delays were 32.0, 54.3, 76.1, 97.8, and 119.6 ms, corresponding to multiples of $1/J_{NH}$.

NMR Data Processing and Analysis. All data were processed using nmrPipe (*48*). The raw data were apodized using Lorentz-to-Gauss transformation in the ^{1}H dimension and shifted sine bell extending from $\pi/3$ to π in the ^{15}N dimension. The final size of each matrix was 4096 × 512 real points after zero filling and Fourier transformation. In the case of the L12 relaxation data, peak intensities were evaluated as peak integrals in a box of 5 × 3 points. The uncertainty of the peak integrals was estimated as the standard deviation of the baseline noise, multiplied by the square root of the box size. The relaxation data were analyzed using simplex optimization routines implemented using Matlab. Monoexponential decay curves were fitted to the experimental relaxation data. Standard errors in the optimized parameters were estimated from Monte Carlo simulations using 200 synthetic data sets based on peak uncertainties. Line widths were determined from data apodized using a 10 Hz line broadening and zero-filling to 2048 points, followed by Lorentzian line shape fitting using nlinLS (*48*); 10 Hz was subtracted from the result. In the case of the HSQC spectra of the 50S and 70S ribosomal units, peak intensities were evaluated as two-dimensional integrals using nlinLS (*48*). The number of CTD copies that can be observed in the 70S HSQC experiment was determined on the basis of cross-peak volumes from the 30S subunit and the CTD that have comparable line widths in both dimensions. These peaks occurred in spectral

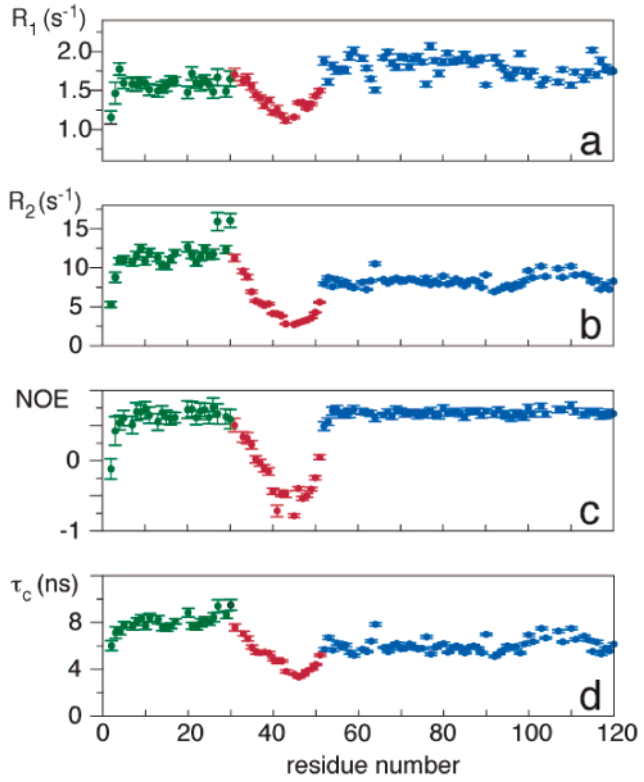

FIGURE 1: ^{15}N relaxation data for the isolated L12 dimer: (a) R_1, (b) R_2, (c) {^{1}H}−^{15}N NOE, and (d) τ_c. Data are plotted against the protein sequence. The error bars represent one standard deviation in the optimized parameters. The data for the NTD, hinge region, and the CTD are shown in green, red, and blue, respectively.

regions that are typical for intact peptide bonds (see Figure 2c). Using resonances from the 30S subunit as an internal reference implies that the derived copy number should be taken as an upper limit, because the 30S subunit could potentially be less than fully populated with its constituent proteins.

RESULTS

Isolated L12: Three Rigid Ellipsoids Joined by Flexible Hinges. Panels a−c of Figure 1 show the ^{15}N longitudinal (R_1) and transverse relaxation rates (R_2) and {^{1}H}−^{15}N nuclear Overhauser enhancements (NOEs) for the isolated L12 dimer, respectively. These data clearly discern three different regions characterized by distinct dynamics. The different regions map perfectly to the NTD, the hinge region, and the CTD. The weighted means for the NTD and CTD are as follows: $\langle R_1 \rangle = 1.6 \pm 0.1$ and 1.8 ± 0.1 s^{-1}, $\langle R_2 \rangle = 11.0 \pm 1.8$ and 8.2 ± 0.7 s^{-1}, and $\langle$NOE$\rangle = 0.62 \pm 0.14$ and 0.68 ± 0.04, respectively, consistent with well-ordered, globular structures. In sharp contrast to the compact NTD and CTD, the hinge region displays low R_1 and R_2 relaxation rates, as well as the heteronuclear NOEs, indicating that the backbone amide N−H bond vectors experience large amplitude fluctuations. These data directly demonstrate that the hinge region is highly flexible and unstructured in solution.

The rotational diffusion correlation time (τ_c) can be calculated on a per-residue basis from the R_2/R_1 ratio (Figure 1d). The local τ_c depends on the orientation of the N−H bond vector in the principal axis frame of the rotational diffusion tensor, and on the principal components of the

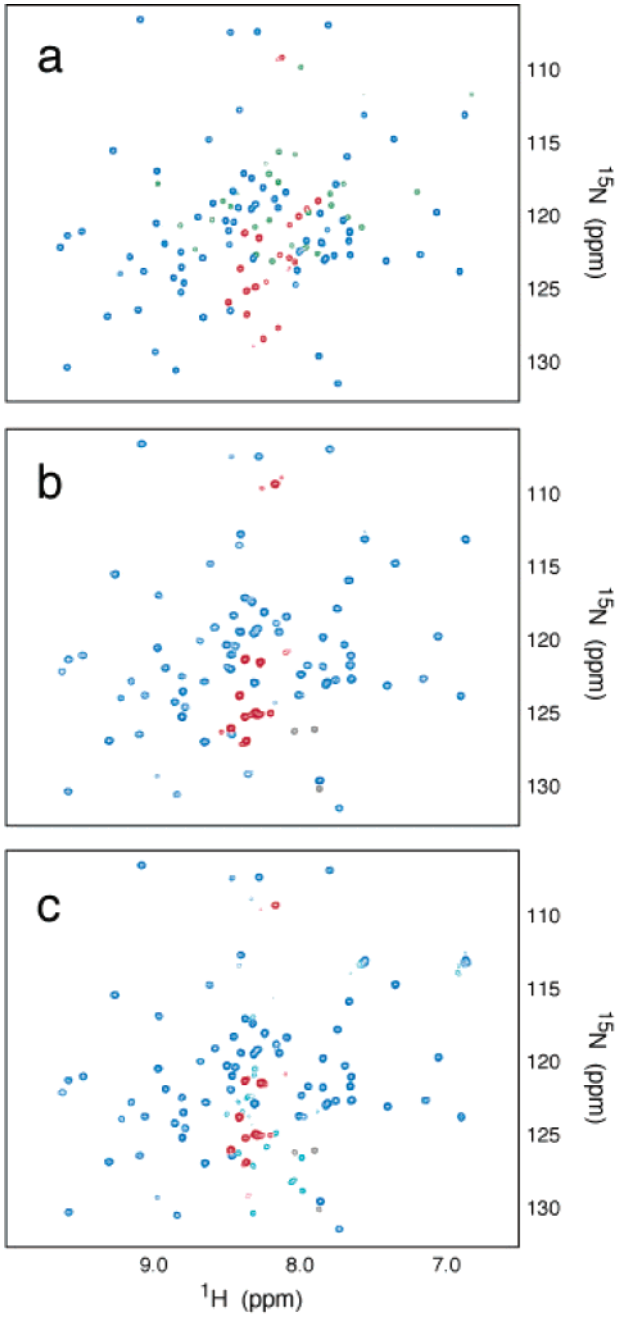

FIGURE 2: ^{1}H−^{15}N HSQC spectra of the isolated L12 dimer and ribosomes: (a) the isolated L12 dimer, (b) the 50S ribosomal subunit, and (c) the intact 70S ribosome. Cross-peaks belonging to the different domains of L12 are shown in green for the NTD, red for the hinge region, and blue for the CTD. Cross-peaks belonging to protein components of the 30S subunit are shown in cyan. Three intense cross-peaks in the 50S and 70S spectra are shown in gray; the chemical shifts and narrow line widths indicate that these most likely correspond to degradation products.

latter. The residues in the NTD have consistently higher values of τ_c than those in the CTD, even though the NTD dimer has a slightly lower molecular weight (M_r = 6910 Da) than the individual CTD (M_r = 7033 Da). Using the three-dimensional structure of the CTD (*36*, *37*), the relaxation data for this domain can be described well by an axially symmetric diffusion tensor with a global effective rotational correlation time (τ_c) of 5.9 ns and an anisotropy factor (D_{par}/D_{per}) of 1.84 (where D_{par} and D_{per} are the principal components of the diffusion tensor). This value corresponds to a

diffusion tensor that is significantly more anisotropic than expected for the isolated CTD, showing that the rotational diffusion of the CTD is restrained in the dimer. The NTD displays rather uniform values of τ_c, which is expected for helices where all N−H bond vectors have approximately the same orientation. Because of the limited number of different bond vector orientations, the degree of rotational anisotropy of the NTD cannot be determined. The rotational diffusion of the NTD dimer is described by a global effective correlation time (τ_c) of 8.0 ns, which is approximately 2 times larger than expected for a globular protein of this size at 30 °C. Thus, the rate of rotational diffusion of the NTD dimer is reduced by the CTDs, and vice versa. It has previously been concluded that the difference in line widths between the NTD and CTD reflects a global exchange process within the NTD dimer between at least two different conformations on a time scale of milliseconds (*44*). In contrast, these results indicate that the difference in R_2 between the NTD and CTD is dominated by rotational diffusion. This is corroborated by measurements of η_{xy}, which, in contrast to R_2, does not include exchange contributions (*47*). The values of η_{xy} exhibit dispersion along the protein sequence that is comparable to that observed for R_2 (data not shown). The weighted mean values for the NTD and CTD ($\langle\eta_{xy}\rangle$) are 6.8 ± 1.0 and 5.6 ± 0.7 s^{-1}, respectively. In the absence of conformational exchange, the ratio ρ (R_2/η_{xy}) depends primarily on structural parameters that are expected to exhibit limited variability between different residues, yielding an average ρ value of 1.3 ± 0.1, as calculated using literature data (*49*). The weighted mean values for the NTD and CTD ($\langle\rho\rangle$) are 1.59 ± 0.19 and 1.45 ± 0.10, respectively, demonstrating that exchange broadening is not significant. Very recently, a parallel study was reported by Arseniev and co-workers (*38*), which agrees well with our conclusions.

Amide ^{1}H Exchange Shows that the Hinge Is Solvent-Exposed. Fast exchange of amide protons with solvent water is manifested as cross-peaks between the HN and H_2O resonances in a 3D ^{15}N−^{1}H TOCSY-HSQC spectrum. Such cross-peaks are observed for residues in unstructured and solvent-exposed areas. These include the N-terminus (residues 1−5), several turns throughout the molecule (residues 16, 61−65, 80, 81, and 93), and the hinge region (residues 33−52). These results are perfectly congruent with those reported above, and demonstrate that the amide protons in the hinge region are not protected from exchange with the solvent.

The ^{1}H−^{15}N HSQC Spectrum of the Ribosome Reveals Mobile L12 CTDs. High-resolution liquid state NMR spectroscopy is not generally expected to yield useful information about particles 2.3 MDa in size. Nonetheless, the ^{1}H−^{15}N HSQC spectrum of the intact (70S) ribosome reveals a number of well-defined cross-peaks that derive from mobile protein components of the ribosome. Figure 2 shows the ^{1}H−^{15}N HSQC spectra of the isolated L12 dimer (a), the 50S subunit (b), and the intact 70S ribosome (c), with color-coded cross-peaks from the different domains of L12 and other protein components of the ribosome. It is clear from Figure 2 that the majority of the cross-peaks that can be observed for the ribosome arises from the CTD of L12. Comparison of HSQC spectra of the 50S (Figure 2b) and 70S particles (Figure 2c) reveals that cross-peaks arising from protein components of the ribosome other than L12 are present

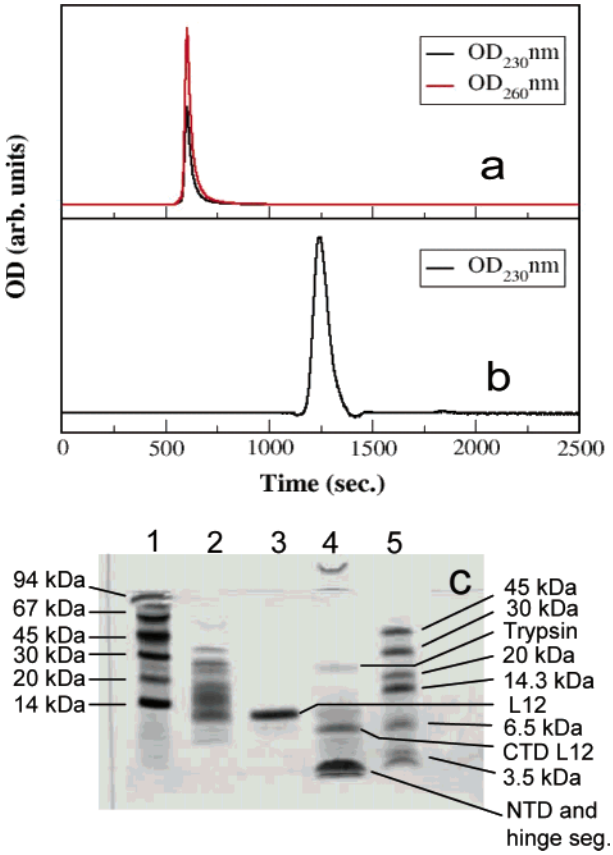

FIGURE 3: Size-exclusion chromatography (a and b) and SDS−PAGE analysis (c) of the NMR samples. Chromatograms of (a) 70S ribosomes and (b) L12 dimer, both at the same concentration used in the NMR studies. (c) High-density Phast gel stained with Coomassie: lane 1, molecular markers; lane 2, 70S ribosome; lane 3, L12; lane 4, trypsin-digested L12 showing the positions of the CTD and NTD; and lane 5, low-molecular weight rainbow markers.

exclusively in the 70S spectrum, and thus correspond to proteins in the 30S subunit. In Figure 2c, these additional cross-peaks are colored cyan. Size-exclusion chromatography and SDS−PAGE showed that the 70S NMR sample did not contain any significant amount of detached L12 dimers or free CTDs originating from proteolytic degradation (Figure 3). Likewise, the high activity of the ribosomes (>85%, as measured by *in vitro* dipeptide synthesis) indicates that they are intact. Thus, the ^{1}H−^{15}N resonances observed in the HSQC spectrum derive from ribosome-bound L12.

The excellent agreement in chemical shifts between isolated and ribosome-bound L12 obviates the need to assign the NMR spectrum of the latter *de novo*. A single set of cross-peaks is observed for residues 40−120 of ribosome-bound L12, indicating that the average structure is identical for all of the copies that contribute to the observed cross-peaks (see further below). As shown in panels a and b of Figure 4, the chemical shift differences between the isolated and ribosome-bound L12 are insignificant, except for residues in the hinge region. The close correspondence in the chemical shifts of the CTD in isolated and ribosome-bound L12 directly indicates that the environment of the CTD is identical in the two states, arguing that the CTD extends away from the ribosome and is surrounded by solvent. The chemical shifts of the hinge residues are increasingly affected the closer they are in sequence to the N-terminus. These minor shift differences suggest that the relative populations of the

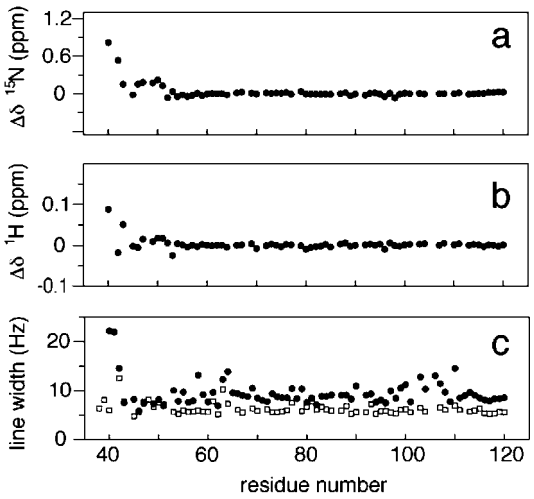

FIGURE 4: Comparison of chemical shifts and line widths for L12 in the isolated dimer and the 70S ribosome: (a) ^{15}N chemical shift differences between the two states, (b) ^{1}H chemical shift differences, and (c) ^{15}N line widths of L12 in the isolated dimer (□) and the 70S ribosome (●).

multiple conformations sampled by the hinge residues are slightly different in the isolated and ribosome-bound states. Further evidence is provided by the observation that the relative populations of the cis and trans isomers of the Gly43−Pro44 peptide bond are more skewed in the ribosome-bound state, as gauged from the relative peak intensities of the two isomers. The chemical shifts of residues 40−120 are virtually identical in the spectra of the 50S and 70S particles, with no shift differences being larger than 0.01 ppm. This indicates that the 30S subunit does not influence the conformation of residues 40−120 of the observable CTDs to any significant extent. Together, these results show that the 50S subunit imparts steric constraints on the conformation of the L12 hinge region, while the 30S subunit does not. No cross-peaks are observed for the NTD and hinge residues 32−39, indicating that the effective rotational diffusion is slow for these segments when they are bound to the ribosome.

Figure 4c shows a comparison of ^{15}N line widths in the HSQC spectra of isolated and ribosome-bound L12. The average values are 6.3 ± 0.8 and 9.3 ± 1.6 Hz, respectively. The average line width is larger in the ribosome-bound state, indicating that the degree of rotational diffusion of the CTD is reduced compared to that of the isolated L12 dimer. This result reconfirms that the CTD cross-peaks observed in the 70S spectrum do not arise from L12 dimers that have dissociated from the ribosome. Residues in the N-terminal part of the hinge region in ribosome-bound L12 exhibit increased line widths, as expected from the reduced internal rotational averaging experienced by these residues that are closest to the NTD.

Two Copies of L12 Are Mobile on the Ribosome. We estimated the number of copies of L12 that contribute to the resonances that are visible in the ^{1}H−^{15}N HSQC spectrum of the 70S ribosome by comparing peak intensities from L12 with those from well-resolved residues in the 30S subunit. The line widths of L12 and the 30S components are comparable, indicating that relative peak intensities may be safely interpreted in terms of the relative populations of these proteins, even though the HSQC experiments did not allow for complete recovery of equilibrium magnetization between transients. The average intensity of CTD residues in ribosome-bound L12 is 2.2 ± 0.3, while the corresponding value for the 30S components is 1.0 ± 0.18. Since all proteins in the 30S subunit are present in single copies, our result indicates that 2.2 ± 0.5 copies of L12 have mobile CTDs when bound to the ribosome. Strictly, this value should be regarded as an upper limit, because the occupancy of the 30S proteins on the ribosome may be less than 100%.

DISCUSSION

Several important conclusions about the L12 dimer can be drawn from the ^{15}N relaxation data obtained for isolated L12. First, they clearly show that the isolated L12 dimer forms a symmetric and extended structure in which the NTDs and CTDs have different rotational diffusion properties. Persistent contacts do not exist between the two CTDs in the dimer, or between a single CTD and the NTD dimer. Second, the results prove that both hinges are unstructured and highly flexible, resulting in a poorly defined orientation of the CTDs relative to the NTD dimer. Third, the NTD dimer is a rigid structure that does not exhibit any significant extent of millisecond time scale exchange between multiple conformations in the dimer. This observation reconfirms that the NTDs are responsible for the strong dimer interaction of L12. Very similar conclusions were reached in the parallel study conducted by Arseniev and co-workers (*38*).

The close agreement between the chemical shifts of every backbone amide group of the CTD in isolated and ribosome-bound L12 directly shows that the structure of the entire CTD remains the same whether it is free or ribosome-bound. Hinge residues 40−51 are also visible in the HSQC spectrum of the ribosome, indicating that this segment does not form an extension of the second α-helix of the NTD. This structure is very different from the crystal structure (*37*) in that the hinge is flexible, and there are no persistent contacts between the CTD and other parts of L12. The NTDs are apparently rigidly attached to the ribosome, as expected (*30*−*32*). The observation that only the second half of the hinge region is visible in the ^{1}H−^{15}N HSQC spectrum reflects the fact that the effective rotational averaging increases with the distance from the ribosome core along the flexible peptide chain; not until residue 40 is rotational averaging sufficiently extensive to produce narrow NMR lines.

There have been several attempts to describe the dimerization mode of L12. In their report describing the crystal structure of L12 from *T. maritima* (65% of the sequence identical with that of the *E. coli* protein), Wahl and co-workers discussed two possible dimerization modes (*37*), corresponding to a compact "core dimer" (or parallel dimer) and a "peripheral dimer" (or antiparallel dimer). In this crystal structure, two full-length molecules form the parallel dimer through interactions that involve mainly a well-structured α-helix formed by residues 30−53 (corresponding to the hinge region), and some additional NTD−NTD and NTD−CTD contacts, yielding a highly compact core dimer, in stark contrast to the results presented here, as well as previous observations by NMR and small-angle X-ray scattering studies of L12 in solution (*35*, *44*). The alternative peripheral dimer involves one full-length molecule and an

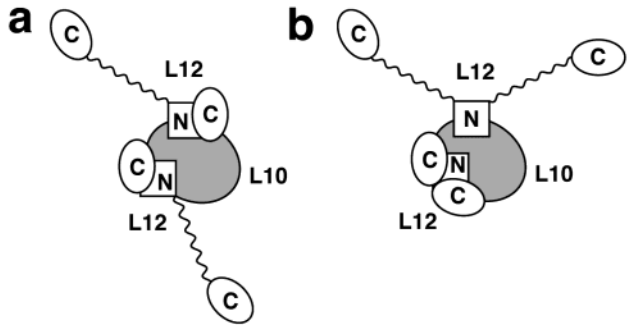

FIGURE 5: Two possible models of L12 dimers bound on the ribosome. (a) Both L12 dimers have one extended and one retracted CTD. (b) One L12 dimer has both CTDs extended, while the other dimer has both CTDs retracted.

N-terminal fragment arranged in antiparallel fashion. Two full-length molecules cannot form a symmetric antiparallel dimer with the hinge segments folded into helices, since this would lead to a severe steric clash (*37*). The recent NMR structure (*38*) reveals an antiparallel dimer similar to the peripheral dimer of the crystal structure (*37*), but with both hinges unstructured. On the basis of the crystal structure, Sanyal and Liljas (*11*) proposed an alternative model for an antiparallel L12 dimer, in which one of the hinge regions forms an α-helix whereas the other is unstructured. Thus, in this asymmetric dimer model, one molecule is retracted into a compact conformation while the other is extended. Possibly, interactions with L10 and other ribosome components may favor the transition of a single hinge in each L12 dimer from the flexible conformation observed in solution to the helical conformation observed in the crystal. Such ribosome-induced conformational changes are expected to have functional consequences. Specifically, they can explain how the CTD is able to contact different parts of the ribosome that are located both in the vicinity of L10 and at more distant sites. Additional interactions with translation factors may induce further conformational changes in L12. However, the conformation and the relative orientation of the two L12 dimers on the ribosome remain elusive. The results presented here narrow the scope of the possible arrangements of L12. Comparing the peak intensities of the CTD residues of L12 with those of the observable 30S components, we conclude that the extended stalk of the ribosome includes at most two copies of the L12 CTD, which are highly mobile in the absence of translation factors. The average structures of these two copies are identical, with respect both to each other and to the isolated protein, as are their interactions with the ribosome. The other two copies of the CTD appear to be tightly bound to the ribosome. These results do not provide information about which two of the four L12 copies have mobile CTDs when they are bound to the ribosome. Two possibilities exist, as depicted in Figure 5. Either the two mobile copies belong to two different dimers (Figure 5a), or they belong to the same dimer (Figure 5b). Intriguingly, the former possibility (Figure 5a) is in full agreement with the model suggested previously (*11*). In contrast, the model represented by Figure 5b requires that at least one of the molecules with retracted CTD have a structure different from the compact helical one observed in the crystal (due to the steric constraints mentioned above).

The novel observations presented herein should provide important points of reference for model building and interpretation of three-dimensional reconstructions based on cryoelectron microscopy images. Further studies are required to address the detailed arrangement of L12 dimers on the ribosome, and to investigate possible structural rearrangements of L12 upon binding of translation factors.

REFERENCES

1. Ban, N., Nissen, P., Hansen, J., Moore, P. B., and Steitz, T. A. (2000) The complete atomic structure of the large ribosomal subunit at 2.4 Å resolution, *Science 289*, 905−920.
2. Wimberly, B. T., Brodersen, D. E., Clemons, W. M., Jr., Morgan-Warren, R. J., Carter, A. P., Vonrhein, C., Hartsch, T., and Ramakrishnan, V. (2000) Structure of the 30S ribosomal subunit, *Nature 407*, 327−339.
3. Schluenzen, F., Tocilj, A., Zarivach, R., Harms, J., Gluehmann, M., Janell, D., Bashan, A., Bartels, H., Agmon, I., Franceschi, F., and Yonath, A. (2000) Structure of functionally activated small ribosomal subunit at 3.3 Å resolution, *Cell 102*, 615−623.
4. Gabashvili, I. S., Agrawal, R. K., Spahn, C. M., Grassucci, R. A., Svergun, D. I., Frank, J., and Penczek, P. (2000) Solution structure of the *E. coli* 70S ribosome at 11.5 Å resolution, *Cell 100*, 537−549.
5. Yusupov, M. M., Yusupova, G. Z., Baucom, A., Lieberman, K., Earnest, T. N., Cate, J. H., and Noller, H. F. (2001) Crystal structure of the ribosome at 5.5 Å resolution, *Science 292*, 883−896.
6. Wriggers, W., Agrawal, R. K., Drew, D. L., McCammon, A., and Frank, J. (2000) Domain motions of EF-G bound to the 70S ribosome: insights from a hand-shaking between multi-resolution structures, *Biophys. J. 79*, 1670−1678.
7. Valle, M., Zavialov, A., Li, W., Stagg, S. M., Sengupta, J., Nielsen, R. C., Nissen, P., Harvey, S. C., Ehrenberg, M., and Frank, J. (2003) Incorporation of aminoacyl-tRNA into the ribosome as seen by cryo-electron microscopy, *Nat. Struct. Biol. 10*, 899−906.
8. Valle, M., Zavialov, A., Sengupta, J., Rawat, U., Ehrenberg, M., and Frank, J. (2003) Locking and unlocking of ribosomal motions, *Cell 114*, 123−134.
9. Wilson, K. S., and Noller, H. F. (1998) Molecular movement inside the translational engine, *Cell 92*, 337−349.
10. Ogle, J. M., Carter, A. P., and Ramakrishnan, V. (2003) Insights into the decoding mechanism from recent ribosome structures, *Trends Biochem. Sci. 28*, 259−266.
11. Sanyal, S. C., and Liljas, A. (2000) The end of the beginning: structural studies of ribosomal proteins, *Curr. Opin. Struct. Biol. 10*, 633−636.
12. Kischa, K., and Möller, W. (1971) Reconstitution of a GTPase activity by a 50S ribosomal protein from *E. coli*, *Nat. New Biol. 233*, 62−63.
13. Möller, W., Schrier, P. I., Maassen, J. A., Zantema, A., Schop, E., Reinalda, H., Cremers, A. F., and Mellema, J. E. (1983) Ribosomal proteins L7/L12 of *Escherichia coli*. Localization and possible mechanism in translation, *J. Mol. Biol. 163*, 553−573.
14. Savelsbergh, A., Mohr, D., Wilden, B., Wintermeyer, W., and Rodnina, M. V. (2000) Stimulation of GTPase activity of translation elongation factor G by ribosomal protein L7/L12, *J. Biol. Chem. 275*, 890−894.
15. Mohr, D., Wintermeyer, W., and Rodnina, M. V. (2002) GTPase activation of elongation factors Tu and G on the ribosome, *Biochemistry 41*, 12520−12528.
16. Hamel, E., Koka, M., and Nakamoto, T. (1972) Requirement of an *Escherichia coli* 50S ribosomal protein component for effective interaction of the ribosome with T and G factors and with guanosine triphosphate, *J. Biol. Chem. 247*, 805−814.
17. Pettersson, I., and Kurland, C. G. (1980) Ribosomal protein L7/L12 is required for optimal translation, *Proc. Natl. Acad. Sci. U.S.A. 77*, 4007−4010.
18. Kirsebom, L. A., Amons, R., and Isaksson, L. A. (1986) Primary structures of mutationally altered ribosomal protein L7/L12 and their effects on cellular growth and translation accuracy, *Eur. J. Biochem. 156*, 669−675.
19. Wahl, M. C., and Möller, W. (2002) Structure and function of the acidic ribosomal stalk proteins, *Curr. Protein Pept. Sci. 3*, 93−106.

20. Agrawal, R. K., Heagle, A. B., Penczek, P., Grasucci, R. A., and Frank, J. (1999) EF-G dependent GTP hydrolysis induces translocation accompanied by large conformational changes in the 70S ribosome, *Nat. Struct. Biol. 6*, 643−647.
21. Harms, J., Schluenzen, F., Zarivach, R., Bashan, A., Gat, S., Agmon, I., Bartels, H., Franceschi, F., and Yonath, A. (2001) High-resolution structure of the large ribosomal subunit from a mesophilic eubacterium, *Cell 107*, 679−688.
22. Gudkov, A. T., Gongadze, G. M., Bushuev, V. N., and Okon, M. S. (1982) Proton nuclear magnetic resonance study of the ribosomal protein L7/L12 in situ, *FEBS Lett. 138*, 229−232.
23. Cowgill, C. A., Nichols, B. G., Kenny, J. W., Butler, P., Bradbury, E. M., and Traut, R. R. (1984) Mobile domains in ribosomes revealed by proton nuclear magnetic resonance, *J. Biol. Chem. 259*, 15257−15263.
24. Hamman, B. D., Oleinikov, A. V., Jokhadze, G. G., Traut, R. R., and Jameson, D. M. (1996) Rotational and conformational dynamics of *Escherichia coli* ribosomal protein L7/L12, *Biochemistry 35*, 16672−16679.
25. Gudkov, A. T., and Gongadze, G. M. (1984) The L7/L12 proteins change their conformation upon interaction of EF-G with ribosomes, *FEBS Lett. 176*, 32−36.
26. Stark, H., Rodnina, M. V., Rinke-Appel, J., Brimacombe, R., Wintermeyer, W., and van Heel, M. (1997) Visualization of elongation factor Tu on the *Escherichia coli* ribosome, *Nature 389*, 403−406.
27. Traut, R. R., Oleinikov, A. V., Makarov, E., Jokhadze, G., Perroud, B., and Wang, B. (1993) in *The translational apparatus: structure, function, evolution* (Nierhaus, K. H., Franceschi, F., Subramanian, A. R., Erdmann, V. A., and Wittmann-Liebold, B., Eds.) pp 521−532, Plenum Publishing Corp., New York.
28. Olson, H. M., Sommer, A., Tewari, D. S., Traut, R. R., and Glitz, D. G. (1986) Localization of two epitopes of protein L7/L12 to both the body and stalk of the large ribosomal subunit. Immune electron microscopy using monoclonal antibodies, *J. Biol. Chem. 261*, 6924−6932.
29. Dey, D., Bochkariov, D. E., Jokhadze, G., and Traut, R. R. (1998) Cross-linking of selected residues in the N- and C-terminal domains of *Escherichia coli* protein L7/L12 to other ribosomal proteins and the effect of elongation factor Tu, *J. Biol. Chem. 273*, 1670−1676.
30. van Agthoven, A. J., Maassen, J. A., Schrier, P. I., and Möller, W. (1975) Inhibition of EF-G dependent GTPase by an amino-terminal fragment of L7/L12, *Biochem. Biophys. Res. Commun. 64*, 1184−1191.
31. Gudkov, A. T., and Behlke, J. (1978) The N-terminal sequence of protein L7/L12 is responsible for its dimerization, *Eur. J. Biochem. 90*, 309−312.
32. Koteliansky, V. E., Domagatsky, S. P., and Gudkov, A. T. (1978) Dimer state of protein L7/L12 and EF-G-dependent reactions of ribosomes, *Eur. J. Biochem. 90*, 319−323.
33. Gudkov, A. T., Bubenenko, M. G., and Gryaznova, O. I. (1991) Overexpression of L7/L12 protein with mutations in its flexible region, *Biochimie 73*, 1387−1389.
34. Bubunenko, M. G., Chuikov, S. V., and Gudkov, A. T. (1992) The length of the interdomain region of the L7/L12 protein is important for its function, *FEBS Lett. 313*, 232−234.
35. Osterberg, R., Sjoberg, B., Pettersson, I., Liljas, A., and Kurland, C. G. (1977) Small-angle X-ray scattering study of the protein complex of L7/L12 and L10 from *Escherichia coli* ribosomes, *FEBS Lett. 73*, 22−24.
36. Leijonmarck, M., and Liljas, A. (1987) Structure of the C-terminal domain of the ribosomal protein-L7 protein-L12 from *Escherichia coli* at 1.7 Å, *J. Mol. Biol. 195*, 555−580.
37. Wahl, M. C., Bourenkov, G. P., Bartunik, H. D., and Huber, R. (2000) Flexibility, conformational diversity and two dimerization modes in complexes of ribosomal protein L12, *EMBO J. 19*, 174−186.
38. Bocharov, E. V., Sobol, A. G., Pavlov, K. V., Korzhnev, D. M., Jaravine, V. A., Gudkov, A. T., and Arseniev, A. S. (2004) From structure and dynamics of protein L7/L12 to molecular switching in ribosome, *J. Biol. Chem.* (in press).
39. Bocharov, E. V., Gudkov, A. T., Budovskaya, E. V., and Arseniev, A. S. (1998) Conformational independence of N- and C-domains in ribosomal protein L7/L12 and in the complex with protein L10, *FEBS Lett. 423*, 347−350.
40. Oleinikov, A. V., Perroud, B., Wang, B., and Traut, R. R. (1993) Structural and functional domains of *Escherichia coli* ribosomal-protein L7/L12. The hinge region is required for activity, *J. Biol. Chem. 268*, 917−922.
41. Rodnina, M. V., and Wintermeyer, W. (1995) GTP consumption of elongation factor Tu during translation of heteropolymeric mRNAs, *Proc. Natl. Acad. Sci. U.S.A. 92*, 1945−1949.
42. Ehrenberg, M., Bilgin, N., and Kurland, C. G. (1990) Design and use of a fast and accurate in vitro translation system, in *Ribosomes and Protein Synthesis: A Practical Approach* (Spedding, G., Ed.) pp 101−128, IRL Press, Oxford, U.K.
43. Spedding, G. (1990) Isolation and analysis of ribosomes from prokaryotes, eukaryotes, and organelles, in *Ribosomes and Protein Synthesis: A Practical Approach* (Spedding, G., Ed.) pp 1−30, IRL Press, Oxford, U.K.
44. Bocharov, E. V., Gudkov, A. T., and Arseniev, A. S. (1996) Topology of the secondary structure elements of ribosomal protein L7/L12 from *E. coli* in solution, *FEBS Lett. 379*, 291−294.
45. Marion, D., Kay, L. E., Sparks, S. W., Torchia, D. A., and Bax, A. (1989) Three-dimensional heteronuclear NMR of N-15-labeled proteins, *J. Am. Chem. Soc. 111*, 1515−1517.
46. Farrow, N. A., Muhandiram, R., Singer, A. U., Pascal, S. M., Kay, C. M., Gish, G., Shoelson, S. E., Pawson, T., Forman-Kay, J. D., and Kay, L. E. (1994) Backbone dynamics of a free and a phosphopeptide-complexed src homology 2 domain studied by ^{15}N NMR relaxation, *Biochemistry 33*, 5984−6003.
47. Kroenke, C. D., Loria, J. P., Lee, L. K., Rance, M., and Palmer, A. G. (1998) Longitudinal and transverse ^{1}H-^{15}N dipolar/^{15}N chemical shift anisotropy relaxation interference: Unambiguous determination of rotational diffusion tensors and chemical exchange effects in biological macromolecules, *J. Am. Chem. Soc. 120*, 7905−7915.
48. Delaglio, F., Grzesiek, S., Vuister, G. W., Zhu, G., Pfeifer, J., and Bax, A. (1995) NMRPipe: A multidimensional spectral processing system based on UNIX pipes, *J. Biomol. NMR 6*, 277−293.
49. Åkerud, T., Thulin, E., Van Etten, R. L., and Akke, M. (2002) Intramolecular Dynamics of Low Molecular Weight Protein Tyrosine Phosphatase in Monomer−Dimer Equilibrium Studied by NMR. A Model for Changes in Dynamics upon Target Binding, *J. Mol. Biol. 322*, 137−152.

BI0495331